Statistical Modeling of Co-Channel Interference in a Field of Poisson Distributed Interferers

Kapil Gulati*, Brian L. Evans* and Keith R. Tinsley†
* The University of Texas at Austin, Austin, Texas 78712
Email: {gulati,bevans}@ece.utexas.edu
†Intel Corporation, Santa Clara, CA 95054
Email: keith.r.tinsley@intel.com

***Abstract*—With increasing spatial reuse of the radio spectrum, co-channel interference is becoming a dominant noise source and may severely degrade the communication performance of wireless transceivers. In this paper, we consider the problem of statistical-physical modeling of co-channel interference from an annulus field of Poisson interferers. Our contributions include (1) demonstrating the applicability of the symmetric alpha stable and Middleton Class A distributions in modeling co-channel interference in various topologies of interferers, and (2) deriving analytical conditions on the system parameters for which these distributions accurately model the interference statistics. Through simulation, we compare the decay rate of tail probabilities of the empirical co-channel interference and the symmetric alpha stable, Middleton Class A, and Gaussian models for different topologies of interferers. Practical applications include co-channel interference modeling for various wireless network environments, including *ad hoc* and cellular networks.**

***Index Terms*—Co-channel interference, Poisson processes, Impulse noise, Probability, Stochastic approximation**

I. Introduction

Current and future wireless communication systems require higher spectral usage due to increasing demand in user data rates. One of the principal techniques for efficient spectral usage is to implement a dense spatial reuse of the available radio spectrum. This causes severe co-channel interference, which limits the system performance. Knowledge of the interference statistics is integral to analyzing performance of wireless networks (e.g. outage probability and throughput) [1] and designing receivers with improved communication performance [2]. We have released a freely distributed software toolbox in MATLAB for statistical modeling and mitigation of radio frequency interference [3].

Statistical-physical modeling of co-channel interference in a Poisson field of interferers has been extensively studied in literature [4]–[6]. Much of the prior work, however, considers the interferers to be distributed over the entire plane. Recently, [7], [8] assumed a finite-area field and studied the interference characteristic function and interference moments, respectively. Closed form approximations to the interference characteristic function or amplitude density, however, were not investigated.

In prior work [9], we presented a unified framework to derive the co-channel interference statistics in a Poisson field of interferers distributed over a parametric circular annulus region. In this paper, we extend the work in [9] for complex baseband interference and demonstrate the applicability of the symmetric alpha stable (SAS) and Middleton Class A (MCA) model for a wider range of interferer topologies. Analytical constraints on the system parameters for which these distributions accurately model the interference statistics are also derived. When exact statistics cannot be derived in closed form, the paper focuses on accurately modeling the tail probability of the interference.

Throughout this paper, random variables are represented using boldface notation, deterministic parameters are represented using non-boldface type, $\mathbb{E}_{\mathbf{X}}\left\{f(\mathbf{X})\right\}$ denotes the expectation of the function $f(\mathbf{X})$ with respect to the random variable $\mathbf{X}$, and $\mathbb{P}(\cdot)$ denotes the probability of a random event.

II. System Model

Consider a wireless communication system in which the receiver receives a signal of interest in the presence of interfering signals. The interferers are assumed to be distributed over the spatial interference space $\Gamma(r_l, r_h) \subseteq \mathbb{R}^2$, and be potentially infinite in number. The receiver is assumed to employ a single omni-directional antenna and is located at $R_m \in \mathbb{R}^2$ with respect to the origin of the two-dimensional coordinate system. The parametric interference space $\Gamma(r_l, r_h)$ is defined as

$$\Gamma(r_l, r_h) = \left\{x \in \mathbb{R}^2 : r_l \leq \|x\| \leq r_h\right\} \tag{1}$$

where $\|\cdot\|$ denotes the Euclidean norm.

At each sampling time instant, location of the active interferers are assumed to be distributed according to a homogeneous spatial Poisson point process $\Upsilon = \{\mathbf{R}_0, \mathbf{R}_1, \cdots\}$ over the space $\Gamma(r_l, r_h)$ with intensity λ.

The baseband model for the sum interference $\mathbf{Y}$ at the receiver at any time instant can then be represented as

$$\mathbf{Y} = \sum_{i=1}^{\mathbf{K}} \mathbf{r}_i^{-\frac{\gamma}{2}} \mathbf{g}_i \mathbf{X}_i \tag{2}$$

where $\mathbf{K}$ is the random number of active interferers at that time instant, i is the interferer index, $\mathbf{r}_i = \|\mathbf{R}_i - R_m\|$ is the random distance of active interferers from the receiver, γ is the power pathloss exponent, $\mathbf{g}_i$ is the independent and

This research was supported by Intel Corporation.

identically distributed (*i.i.d.*) random fast-fading experienced by each interferer emission, and $\mathbf{X}_i$ are the random baseband emissions from the active interferers.

We assume that all potential interferers have *i.i.d.* symmetric narrowband emissions of the form [10]

$$\mathbf{X}_i = \mathbf{B}_i e^{j\boldsymbol{\phi}_i} = \mathbf{B}_i \cos(\boldsymbol{\phi}_i) + j\mathbf{B}_i \sin(\boldsymbol{\phi}_i) \tag{3}$$

where $\mathbf{B}_i$ is the *i.i.d.* envelope, and $\boldsymbol{\phi}_i$ is the *i.i.d.* random phase of the emissions. Further, we assume that the emerging times of the interferers are uniformly distributed between the sampling times at the receiver. Thus the phase $\boldsymbol{\phi}_i$ of the emissions can be assumed to uniformly distributed on $[0, 2\pi]$.

The fast-fading experienced by the interferer emissions is also assumed to be narrowband of the form

$$\mathbf{g}_i = \mathbf{h}_i e^{j\boldsymbol{\theta}_i} \tag{4}$$

where $\mathbf{h}_i$ is the random amplitude scaling and $\boldsymbol{\theta}_i$ is the random phase variation due to fading. The in-phase and quadrature-phase components of the emissions are assumed to experience uncorrelated fading and thus $\boldsymbol{\theta}_i$ is uniformly distributed on $[0, 2\pi]$. The sum interference in (2) can then be expressed as

$$\mathbf{Y} = \sum_{i=1}^{\mathbf{K}} \mathbf{r}_i^{-\frac{\gamma}{2}} \mathbf{h}_i \mathbf{B}_i \left(\cos(\boldsymbol{\phi}_i + \boldsymbol{\theta}_i) + j\sin(\boldsymbol{\phi}_i + \boldsymbol{\theta}_i)\right). \tag{5}$$

III. Statistical-Physical Modeling

From (5), the joint characteristic function of the in-phase and quadrature-phase components of the sum interference $\mathbf{Y} = \mathbf{Y}_I + j\mathbf{Y}_Q$ can be expressed as

$$\Phi_{\mathbf{Y}_I,\mathbf{Y}_Q}(\omega_I, \omega_Q)$$
$$= \mathbb{E}_{\mathbf{Y}_I,\mathbf{Y}_Q}\left\{e^{j\omega_I \mathbf{Y}_I + j\omega_Q \mathbf{Y}_Q}\right\} \tag{6}$$
$$= \mathbb{E}\left\{e^{j|\overline{\omega}|\sum_{i=1}^{\mathbf{K}} \mathbf{r}_i^{-\frac{\gamma}{2}} \mathbf{h}_i \mathbf{B}_i \cos(\boldsymbol{\phi}_i + \boldsymbol{\theta}_i + \overline{\omega}_\phi)}\right\} \tag{7}$$
$$= \sum_{k=0}^{\infty} \mathbb{E}\left\{e^{j|\overline{\omega}|\sum_{i=1}^{k} \mathbf{r}_i^{-\frac{\gamma}{2}} \mathbf{h}_i \mathbf{B}_i \cos(\boldsymbol{\phi}_i + \boldsymbol{\theta}_i + \overline{\omega}_\phi)} \middle| k \text{ in } \Gamma(r_l, r_h)\right\} \times \mathbb{P}\left(k \text{ in } \Gamma(r_l, r_h)\right) \tag{8}$$

where $\overline{\omega} = [\omega_I, \omega_Q]^T$, $|\overline{\omega}| = \sqrt{\omega_I^2 + \omega_Q^2}$, and $\overline{\omega}_\phi = -\tan^{-1}\left(\frac{\omega_Q}{\omega_I}\right)$. The expectation in (8) is with respect to the set of random variables $\{\mathbf{r}_i, \mathbf{h}_i, \mathbf{B}_i, \boldsymbol{\phi}_i, \boldsymbol{\theta}_i\}$.

Conditioned on the number of interferers present in the space $\Gamma(r_l, r_h)$, the interferer locations are mutually independent and uniformly distributed over this space [11]. Henceforth, we remove the conditioning on the number of interferers from the expectation by noting that the interferers are uniformly distributed in the space $\Gamma(r_l, r_h)$. For *i.i.d.* interferer emissions, the characteristic function can be expressed as

$$\Phi_{\overline{\mathbf{Y}}}(\overline{\omega}) = \sum_{k=0}^{\infty}\left[\mathbb{E}\left\{e^{j|\overline{\omega}|\mathbf{r}^{-\frac{\gamma}{2}}\mathbf{h}\mathbf{B}\cos(\boldsymbol{\phi}+\boldsymbol{\theta}+\overline{\omega}_\phi)}\right\}\right]^k \times \frac{\left[\lambda\pi\left(r_h^2 - r_l^2\right)\right]^k e^{-\lambda\pi\left(r_h^2 - r_l^2\right)}}{k!} \tag{9}$$
$$= e^{\lambda\pi\left(r_h^2 - r_l^2\right)\left(\mathbb{E}\left\{e^{j|\overline{\omega}|\mathbf{r}^{-\frac{\gamma}{2}}\mathbf{h}\mathbf{B}\cos(\boldsymbol{\phi}+\boldsymbol{\theta}+\overline{\omega}_\phi)}\right\}-1\right)} \tag{10}$$

where $\overline{\mathbf{Y}}$ is the set of random variables $\{\mathbf{Y}_I, \mathbf{Y}_Q\}$. By taking the logarithm of $\Phi_{\overline{\mathbf{Y}}}(\overline{\omega})$, and using the identity

$$e^{ja\cos(\phi)} = \sum_{k=0}^{\infty} j^k \epsilon_k J_k(a)\cos(k\phi) \tag{11}$$

where $\epsilon_0 = 1$, $\epsilon_k = 2$ for $k \geq 1$, and $J_k(\cdot)$ denotes the Bessel function of order k, the log-characteristic function is

$$\psi_{\overline{\mathbf{Y}}}(\overline{\omega}) = \lambda\pi\left(r_h^2 - r_l^2\right) \times \left(\mathbb{E}\left\{\sum_{k=0}^{\infty} j^k \epsilon_k J_k\left(|\overline{\omega}|\mathbf{r}^{-\frac{\gamma}{2}}\mathbf{h}\mathbf{B}\right)\cos\left(k(\boldsymbol{\phi}+\boldsymbol{\theta}+\overline{\omega}_\phi)\right)\right\} - 1\right). \tag{12}$$

Since $\boldsymbol{\phi}$ and $\boldsymbol{\theta}$ are uniformly distributed on $[0, 2\pi]$, $\mathbb{E}_{\boldsymbol{\phi},\boldsymbol{\theta}}\left\{\cos\left(k(\boldsymbol{\phi}+\boldsymbol{\theta}+\overline{\omega}_\phi)\right)\right\} = 0$ for $k \geq 1$, and (12) reduces to

$$\psi_{\overline{\mathbf{Y}}}(\overline{\omega}) = \lambda\pi\left(r_h^2 - r_l^2\right)\left(\mathbb{E}_{\mathbf{r},\mathbf{h},\mathbf{B}}\left\{J_0\left(|\overline{\omega}|\mathbf{r}^{-\frac{\gamma}{2}}\mathbf{h}\mathbf{B}\right)\right\} - 1\right). \tag{13}$$

The log-characteristic function derived in (13) holds in general for narrowband interferers distributed over the parametric space $\Gamma(r_l, r_h)$. We now consider the following three cases and further simplify the log-characteristic function.

A. Case I: Interferers distributed over the entire plane ($r_l = 0, r_h \to \infty$)

This scenario corresponds to a decentralized random network where the nodes do not employ any contention-based medium access control (MAC) layer protocol and has been widely studied in literature [4]–[7], [9]. Note that $\|R_m\|$ can be assumed to be zero without any loss in generality of the result. From [9], the log-characteristic function can be expressed as

$$\psi_{\overline{\mathbf{Y}}}(\overline{\omega}) = -|\overline{\omega}|^{\frac{4}{\gamma}}\lambda\pi\mathbb{E}_{\mathbf{h},\mathbf{B}}\left\{\mathbf{h}^{\frac{4}{\gamma}}\mathbf{B}^{\frac{4}{\gamma}}\right\}\int_0^{\infty}\frac{J_1(x)}{x^{\frac{4}{\gamma}}}dx. \tag{14}$$

Equation (14) is the log-characteristic function of an isotropic SAS distribution centered at zero such that

$$\psi_{\mathbf{Y}_I,\mathbf{Y}_Q}(\omega_I, \omega_Q) = -\sigma\left|\sqrt{\omega_I^2 + \omega_Q^2}\right|^{\alpha} \tag{15}$$

where $\alpha = \frac{4}{\gamma}$ is the characteristic exponent ($0 < \alpha < 2$), and $\sigma = \lambda\pi\mathbb{E}_{\mathbf{h},\mathbf{B}}\{\mathbf{h}^\alpha\mathbf{B}^\alpha\}\int_0^\infty \frac{J_1(x)}{x^\alpha}dx$ is the dispersion parameter of the SAS distribution [11].

B. Case II: Interferers distributed over a finite-area annular region ($0 \leq r_l < r_h < \infty$, and $R_m \notin \Gamma(r_l, r_h)$)

This scenario corresponds to interference from local area wireless networks (such as a hotspot) or wireless networks employing contention-based MAC protocols. In [10], Middleton proposed an approximation of the log-characteristic function for $|\overline{\omega}|$ in the neighborhood of zero. From Fourier analysis, the behavior of the characteristic function in neighborhood of zero governs the tail probability of the random envelope. The proposed approximation is based on the identity [10]:

$$\mathbb{E}_{\mathbf{r},\mathbf{h},\mathbf{B}}\left\{J_0\left(|\overline{\omega}|\mathbf{r}^{-\frac{\gamma}{2}}\mathbf{h}\mathbf{B}\right)\right\} = e^{-\frac{|\overline{\omega}|^2\mathbb{E}_{\mathbf{r},\mathbf{h},\mathbf{B}}\left\{\mathbf{r}^{-\gamma}\mathbf{h}^2\mathbf{B}^2\right\}}{4}} \times \left(1 + \boldsymbol{\Lambda}(|\overline{\omega}|)\right). \tag{16}$$

Here, $\mathbf{\Lambda}(|\overline{\omega}|)$ indicates a correction term with the lowest exponent in $|\overline{\omega}|$ of four and is given by

$$\mathbf{\Lambda}(|\overline{\omega}|)=\sum_{k=2}^{\infty}\frac{\left(\mathbb{E}_{\mathbf{Z}}\left\{\mathbf{Z}\right\}\right)^{k}|\overline{\omega}|^{2k}}{2^{2k}k!}\mathbb{E}_{\mathbf{Z}}\left\{{}_1F_1\left(-k;1;\frac{\mathbf{Z}}{\mathbb{E}_{\mathbf{Z}}\left\{\mathbf{Z}\right\}}\right)\right\} \tag{17}$$

where the random variable $\mathbf{Z}=\mathbf{r}^{-\gamma}\mathbf{h}^2\mathbf{B}^2$, and ${}_1F_1\left(a;b;x\right)$ is the confluent hypergeometric function of the first kind, such that $\mathbf{\Lambda}(|\overline{\omega}|)=O(|\overline{\omega}|^4)$ as $|\overline{\omega}|\rightarrow 0$.

Using the identity (16), and approximating $\mathbf{\Lambda}(|\overline{\omega}|)<<1$ for $|\overline{\omega}|$ in the neighborhood of zero, the log-characteristic function in (13) can be expressed as

$$\psi_{\overline{\mathbf{Y}}}(\overline{\omega})=\lambda\pi\left(r_h^2-r_l^2\right)\left(e^{-\frac{|\overline{\omega}|^2\mathbb{E}_{\mathbf{r},\mathbf{h},\mathbf{B}}\left\{\mathbf{r}^{-\gamma}\mathbf{h}^2\mathbf{B}^2\right\}}{4}}-1\right). \tag{18}$$

Equation (18) is the log-characteristic function of a MCA model (without the additive Gaussian component) such that

$$\psi_{\mathbf{Y}_I,\mathbf{Y}_Q}(\omega_I,\omega_Q)=A\left(e^{-\frac{\left(\omega_I^2+\omega_Q^2\right)\Omega_{2A}}{2A}}-1\right) \tag{19}$$

where $A=\lambda\pi\left(r_h^2-r_l^2\right)$ is the overlap index that indicates the impulsiveness of interference, and $\Omega_{2A}=\frac{A\times\mathbb{E}_{\mathbf{r},\mathbf{h},\mathbf{B}}\left\{\mathbf{r}^{-\gamma}\mathbf{h}^2\mathbf{B}^2\right\}}{2}$ is the mean intensity of the interference [10]. Using (19), the joint probability density function can be expressed as

$$f_{\mathbf{Y}_I,\mathbf{Y}_Q}(y_I,y_Q)=e^{-A}\delta(y_I)\delta(y_Q)+\sum_{m=1}^{\infty}\frac{e^{-A}A^m}{m!}\frac{e^{-\frac{\left(y_I^2+y_Q^2\right)}{2\sigma_m^2}}}{\sqrt{2\pi}\sigma_m} \tag{20}$$

where $\sigma_m^2=\frac{m}{A}\Omega_{2A}$ and $\delta(\cdot)$ is the Dirac delta functional.

The correspondence to the MCA distribution is particularly valid for modeling the tail probabilities. From [9], the MCA model provides a good approximation in this scenario when

$$\left|\frac{\mathbb{E}_{\mathbf{r},\mathbf{h},\mathbf{B}}\left\{\mathbf{r}^{-2\gamma}\mathbf{h}^4\mathbf{B}^4\right\}}{4\times\left[\mathbb{E}_{\mathbf{r},\mathbf{h},\mathbf{B}}\left\{\mathbf{r}^{-\gamma}\mathbf{h}^2\mathbf{B}^2\right\}\right]^2}-\frac{1}{2}\right| << 1. \tag{21}$$

C. Case III: Interferers distributed over infinite-area annular region with guard zone (r_l>0, $r_h\rightarrow\infty$, and $R_m\notin\Gamma(r_l,r_h)$)

This scenario corresponds to interference in large-scale random wireless networks employing contention-based MAC protocols. As $r_h\rightarrow\infty$, with high probability, the distance of an interferer from receiver located at R_m can be approximated as $\mathbf{r}=\|\mathbf{R}-R_m\|\approx\|\mathbf{R}\|$, particularly for $\|R_m\|<<r_l$. The distance of each interferer from the receiver thus follows the distribution

$$f_{\mathbf{r}|\mathbf{K}}(r|K)=\begin{cases}\frac{2r}{r_h^2-r_l^2} & \text{if } r_l\leq r\leq r_h,\\ 0 & \text{otherwise.}\end{cases}$$

Expanding the expectation in (13), we have

$$\psi_{\overline{\mathbf{Y}}}(\overline{\omega})=\lim_{r_h\rightarrow\infty}\lambda\pi(r_h^2-r_l^2)\left(\int_{r_l}^{r_h}\mathbb{E}_{\mathbf{h},\mathbf{B}}\left\{J_0\left(|\overline{\omega}|r^{-\frac{\gamma}{2}}\mathbf{h}\mathbf{B}\right)\right\}\times\frac{2r}{r_h^2-r_l^2}dr-1\right). \tag{22}$$

Integrating the above by parts, reordering terms, and noting that $\lim_{r_h\rightarrow\infty}\lambda\pi r_h^2\left(\mathbb{E}_{\mathbf{h},\mathbf{B}}\left\{J_0\left(|\overline{\omega}|r_h^{-\frac{\gamma}{2}}\mathbf{h}\mathbf{B}\right)\right\}-1\right)=0$ for $\gamma>2$, we have

$$\psi_{\overline{\mathbf{Y}}}(\overline{\omega})=-\lambda\pi r_l^2\left(\mathbb{E}_{\mathbf{h},\mathbf{B}}\left\{J_0\left(|\overline{\omega}|r_l^{-\frac{\gamma}{2}}\mathbf{h}\mathbf{B}\right)\right\}-1\right)-\lim_{r_h\rightarrow\infty}\lambda\pi\int_{r_l}^{r_h}\frac{\partial}{\partial r}\left(\mathbb{E}_{\mathbf{h},\mathbf{B}}\left\{J_0\left(|\overline{\omega}|r^{-\frac{\gamma}{2}}\mathbf{h}\mathbf{B}\right)\right\}\right)r^2dr. \tag{23}$$

Invoking the identity (16), approximating $\mathbf{\Lambda}(|\overline{\omega}|)<<1$ for $|\overline{\omega}|$ in the neighborhood of zero, and using Taylor series expansion of e^x, the log-characteristic function reduces to

$$\psi_{\overline{\mathbf{Y}}}(\overline{\omega})=\lambda\pi r_l^2\left[\sum_{k=1}^{\infty}\frac{(-1)^k|\overline{\omega}|^{2k}}{4^kk!}\left(\mathbb{E}\left\{\mathbf{h}^2\mathbf{B}^2\right\}\right)^k r_l^{-\gamma k}\frac{2}{k\gamma-2}\right] \tag{24}$$

valid for $\gamma>2$. Note that unlike (16), the approximation of (23) involves a non-random r. The $\frac{2}{k\gamma-2}$ multiplicative factor inside the summation prevents the log-characteristic function to be expressed in closed form. We thus approximate the function $\frac{2}{k\gamma-2}$ as $\eta e^{\beta k}$ for $k\geq 1$. The parameters η and β are chosen to minimize the weighted mean squared error

$$\{\eta,\beta\}=\arg\min_{\eta,\beta}\sum_{k=1}^{\infty}\left(\frac{2}{k\gamma-2}-\eta e^{\beta k}\right)^2u(k) \tag{25}$$

where $u(k)$ are the weights. The weights should be chosen such that penalty of error is large when k is small since it affects the coefficients of terms with lower order exponents of $|\overline{\omega}|$. In our simulations, we use the weights $u(k)=e^{-k}$. Using this approximation, the log-characteristic function reduces to

$$\psi_{\overline{\mathbf{Y}}}(\overline{\omega})=\lambda\pi r_l^2\eta\left(e^{-\frac{|\overline{\omega}|^2r_l^{-\gamma}e^{\beta}\mathbb{E}_{\mathbf{h},\mathbf{B}}\left\{\mathbf{h}^2\mathbf{B}^2\right\}}{4}}-1\right). \tag{26}$$

Equation (26) is the log-characteristic function of MCA distribution (without the additive Gaussian component) as given in (19) with impulsive index $A=\lambda\pi r_l^2\eta$, and mean intensity $\Omega_{2A}=\frac{A\times r_l^{-\gamma}e^{\beta}\mathbb{E}_{\mathbf{h},\mathbf{B}}\left\{\mathbf{h}^2\mathbf{B}^2\right\}}{2}$.

The choice of the functional form $\eta e^{\beta k}$ to approximate the function $\frac{2}{k\gamma-2}$ for $k\geq 1$ was chosen since (a) it provides a good approximation and enables the log-characteristic function to be expressed in closed form, and (b) provides two free parameters $\{\eta,\beta\}$ such that η affects only the overlap index A, while β affects only the variance $\sigma_m^2=\frac{m}{A}\Omega_{2A}$ of individual components of the Gaussian mixture form of MCA model.

Analogous to *Case II*, a first-order measure of the accuracy of the approximation can be expressed by comparing the coefficient of $|\overline{\omega}|^4$ term in the true log-characteristic function (23) against that in the approximated log-characteristic function (26). The MCA distribution provides a good approximation to co-channel interference statistics in this scenario when

$$\left|\left(\frac{\left[\mathbb{E}_{\mathbf{h},\mathbf{B}}\left\{\mathbf{h}^2\mathbf{B}^2\right\}\right]^2}{64}\right)\left(\frac{2}{2\gamma-2}-2\eta e^{2\beta}\right)+\left(\frac{\mathbb{E}_{\mathbf{h},\mathbf{B}}\left\{\mathbf{h}^4\mathbf{B}^4\right\}}{128}\right)\left(\frac{2}{2\gamma-2}\right)\right|<<\left|\frac{\left[\mathbb{E}_{\mathbf{h},\mathbf{B}}\left\{\mathbf{h}^2\mathbf{B}^2\right\}\right]^2}{32}\eta e^{2\beta}\right|. \tag{27}$$

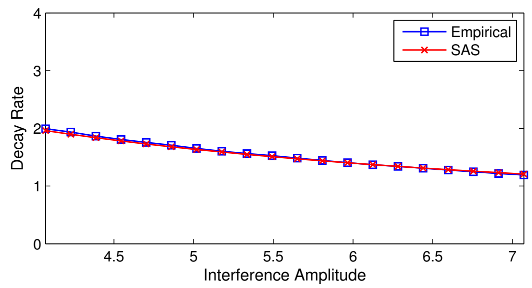

Fig. 1: Decay rates for tail probabilities of simulated co-channel interference and the symmetric alpha stable (SAS) model for *Case I* ($r_l = 0, r_h = \infty, \mathbf{B} = 5$). The Middleton Class A and Gaussian models are not suitable in this scenario as the mean intensity $\Omega_{2A} \to \infty$.

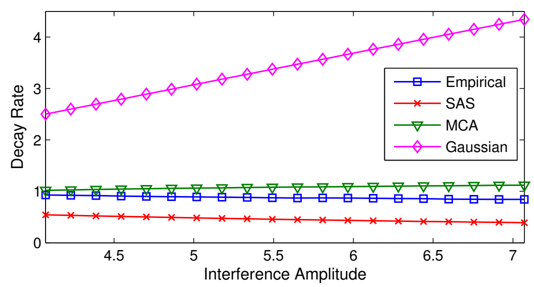

Fig. 2: Decay rates for tail probabilities of simulated co-channel interference and the symmetric alpha stable (SAS), Middleton Class A (MCA), and Gaussian models for *Case II* ($r_l = 20, r_h = 40, \|R_m\| = 4, \mathbf{B} = 1600$). MCA has the best match to the empirical (simulated) co-channel interference.

IV. Simulation Results

Using the model discussed in Section II, we apply Monte-Carlo numerical techniques to simulate the co-channel interference observed at the receiver in various wireless network environments based on (5). At each sample instant, the location of the active interferers is generated as a realization of a spatial Poisson point process with intensity $\lambda = 10^{-4}$ within the region $\Gamma(r_l, r_h)$. Parameter values for r_l, r_h, and R_m change according to the network environment under consideration.

In our simulations, we assume a power path-loss exponent $\gamma = 4$ and Rayleigh fading ($\mathbf{h}$) with unit energy. The amplitude of the interferer emissions, $\mathbf{B}$, was chosen as a constant for a particular wireless environment such that the tail probability, $\mathbb{P}(\|\mathbf{Y}\| > y)$, at an amplitude threshold of $y = 7$ is of the order of 10^{-4}. The empirical distribution of co-channel interference is estimated from 100000 samples of the received interference using kernel smoothed density estimators.

Accuracy of the statistical-physical models for co-channel interference is established by comparing the empirical and interference model tail probabilities. We compare the asymptotic decay rates of the tail probabilities given by

$$\rho\left(y\right) = -\frac{\log\left(\mathbb{P}(\|\mathbf{Y}\| > y)\right)}{y} \tag{28}$$

where $\rho(y)$ is the asymptotic decay rate at interference amplitude y. The decay rate is the rate at which the tail probability asymptotically approaches zero.

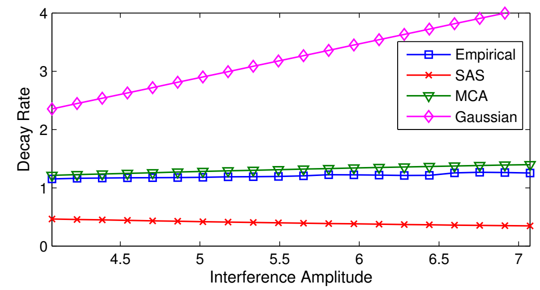

Fig. 3: Decay rates for tail probabilities of simulated co-channel interference and the symmetric alpha stable (SAS), Middleton Class A (MCA), and Gaussian models for *Case III* ($r_l = 30, r_h = \infty, \|R_m\| = 4, \mathbf{B} = 2200$). From (25), $\{\eta, \beta\} = \{2.781, -1.025\}$ for $\gamma = 4$ and $u(k) = e^{-k}$. MCA has the best match to the empirical (simulated) co-channel interference.

Figs. 1, 2, and 3 compare the decay rates of the empirical distribution with the statistical models for *Case I*, *Case II*, and *Case III*, respectively. In each scenario, we compare the empirical distribution against the SAS and the MCA distribution with appropriate parameters as derived in Section III. Further, we compare the empirical distribution to a Gaussian distribution with equal variance for all scenarios.

The results demonstrate that the tail probabilities of the co-channel interference in *Case I* are well modeled using a SAS distribution, while the MCA distribution provides a good fit to the tail probabilities in *Case II* and *Case III*. In all scenarios, the Gaussian distribution decays far too quickly to model the impulsive nature of co-channel interference accurately.

References

[1] S. Weber, J. G. Andrews, and N. Jindal, "The effect of fading, channel inversion, and threshold scheduling on ad hoc networks," *IEEE Trans. on Info. Theory*, vol. 53, no. 11, pp. 4127–4149, 2007.

[2] K. Gulati, A. Chopra, R. W. Heath, B. L. Evans, K. R. Tinsley, and X. E. Lin, "MIMO receiver design in the presence of radio frequency interference," in *Proc. IEEE Global Comm. Conf.*, Nov. 30–Dec. 4 2008.

[3] K. Gulati, M. Nassar, A. Chopra, M. DeYoung, N. Aghasadeghi, A. Sujeeth, and B. L. Evans, "Radio frequency interference modeling and mitigation toolbox in MATLAB," Version 1.3, Aug 2009. [Online]. Available: www.ece.utexas.edu/~bevans/projects/rfi/software/

[4] E. S. Sousa, "Performance of a spread spectrum packet radio network link in a Poisson field of interferers," *IEEE Trans. on Info. Theory*, vol. 38, no. 6, pp. 1743–1754, Nov 1992.

[5] X. Yang and A. Petropulu, "Co-channel interference modeling and analysis in a Poisson field of interferers in wireless communications," *IEEE Trans. on Signal Proc.*, vol. 51, no. 1, pp. 64–76, Jan. 2003.

[6] J. Ilow and D. Hatzinakos, "Analytic alpha-stable noise modeling in a Poisson field of interferers or scatterers," *IEEE Trans. on Signal Proc.*, vol. 46, no. 6, pp. 1601–1611, June 1998.

[7] M. Z. Win, P. C. Pinto, and L. A. Shepp, "A mathematical theory of network interference and its applications," *Proc. of the IEEE*, vol. 97, no. 2, pp. 205–230, Feb. 2009.

[8] E. Salbaroli and A. Zanella, "Interference analysis in a Poisson field of nodes of finite area," *IEEE Trans. on Vehicular Tech.*, vol. 58, no. 4, pp. 1776–1783, May 2009.

[9] K. Gulati, A. Chopra, B. L. Evans, and K. R. Tinsley, "Statistical modeling of co-channel interference," in *Proc. IEEE Global Comm. Conf.*, Nov. 30–Dec. 4 2009.

[10] D. Middleton, "Non-Gaussian noise models in signal processing for telecommunications: New methods and results for class A and class B noise models," *IEEE Trans. on Info. Theory*, vol. 45, no. 4, pp. 1129–1149, May 1999.

[11] G. Samorodnitsky and M. S. Taqqu, *Stable Non-Gaussian Random Processes: Stochastic Models with Infinite Variance*, 1994.